MOLECULAR AND CELLULAR BIOLOGY, Jan. 2002, p. 207–220 Vol. 22, No. 1
0270-7306/02/$04.00+0 DOI: 10.1128/MCB.22.1.207–220.2002

Molecular Ordering of the Initial Signaling Events of CD95

Alicia Algeciras-Schimnich,[1] Le Shen,[1] Bryan C. Barnhart,[1] Andrea E. Murmann,[2] Janis K. Burkhardt,[3] and Marcus E. Peter[1]*

The Ben May Institute for Cancer Research[1] and Department of Medicine[2] and Department of Pathology,[3] University of Chicago, Chicago, Illinois 60637

Received 11 June 2001/Returned for modification 17 July 2001/Accepted 9 October 2001

Binding of either ligand or agonistic antibodies to the death receptor CD95 (APO-1/Fas) induces the formation of the death-inducing signaling complex (DISC). We now show that signal initiation of CD95 in type I cells can be further separated into at least four distinct steps. (i) The first step is ligand-induced formation of CD95 microaggregates at the cell surface. (ii) The second step is recruitment of FADD to form a DISC. This step is dependent on actin filaments. (iii) The third step involves formation of large CD95 surface clusters. This event is positively regulated by DISC-generated caspase 8. (iv) The fourth step is internalization of activated CD95 through an endosomal pathway. The latter step is again dependent on the presence of actin filaments. The data indicate that the signal initiation by CD95 is a complex process actively regulated at various levels, providing a number of new drug targets to specifically modulate CD95 signaling.

CD95 (APO-1/Fas) is the best-studied member of the death receptor family (26). We previously demonstrated that CD95 oligomerizes upon triggering, forming sodium dodecyl sulfate (SDS)-stable microaggregates on SDS-polyacrylamide gel electrophoresis (PAGE) (11). This activated receptor recruits the adapter molecule FADD and the initiator caspase 8 to form the death-inducing signaling complex (DISC) (11). Recently, Siegel et al. (37) refined this model by showing that unstimulated CD95 exists as preassociated complexes, and they and others (10, 24) confirmed the initial observation of the formation of SDS-stable aggregates by stimulated CD95 (11). In addition, CD95 has been reported to form clusters at the cell surface in a ligand-dependent fashion either late (43) or, in two other reports, very early (6, 9) after receptor triggering. The relationship between or the kinetic order of all these events—preassociation, formation of SDS-stable microaggregates, formation of the DISC, and the appearance of higher-order receptor clusters, as seen by immunofluorescence microscopy—is unknown.

We have previously described two different CD95 apoptosis pathways (32). In type I cells, caspase 8 is recruited to the DISC, resulting in release of active caspase 8 in quantities sufficient to directly activate caspase 3 (40). However, in type II cells, despite similar expression levels of surface CD95 and signaling molecules, formation of the DISC is so inefficient that only very small quantities of caspase 8 are generated at the cell surface. This amount of caspase 8 is insufficient to process caspase 3, but sufficient to cleave the BH3-only protein Bid (13, 16, 19), resulting in the apoptogenic activation of mitochondria. Therefore, the execution of apoptosis can be inhibited by overexpression of Bcl-2 or Bcl-x_L only in type II cells (32). Recently, a number of transgenic and knockout studies have provided evidence for the existence of the two pathways in vivo (14, 17, 30, 41, 48, 49). In all cases, CD95 apoptosis execution of thymocytes and peripheral T cells was independent of mitochondria, identifying them as type I cells, whereas the liver was found to be a type II tissue that requires the mitochondrial branch of the CD95 pathway to apoptose.

We now show that the efficient formation of the DISC found in type I cells precedes formation of CD95 surface clusters and that clustering is dependent on DISC-generated active caspase 8. We also demonstrate for the first time that during CD95-mediated apoptosis, the CD95-CD95L complex is internalized through an endosomal pathway. The data allow us to distinguish four sequential early signaling events of CD95: (i) ligand-induced formation of receptor microaggregates, (ii) actin-dependent assembly of the DISC, (iii) caspase 8-dependent formation of higher-order surface receptor clusters, and (iv) actin-driven receptor internalization. The data indicate that expression of the surface CD95 receptor and of DISC signaling molecules enables cells to produce small quantities of active caspase 8 at their ligated receptor. However, formation of a DISC that generates large quantities of caspase 8, characteristic of type I cells, and internalization of the activated receptor-ligand complex require actin filaments.

MATERIALS AND METHODS

Cell lines. The B-lymphoblastoid cell line SKW6.4, the pre-B-cell line Boe^R (8), the T-cell line H9, and K50, a full-length human CD95-expressing transfectant of the Burkitt's lymphoma BL-60 (11), were cultured in RPMI 1640 supplemented with 10% fetal calf serum (FCS), 2 mM glutamine, 100 U of penicillin per ml, and 100 μg of streptomycin per ml and maintained in 5% CO_2 at 37°C. SKW6 cells transfected with vector control or Bcl-2 were cultured as described elsewhere (32). The Burkitt's lymphoma BJAB transfected with vector control or FADD-DN (C-FADD) was generated as described previously (35) and cultured in 10% FCS–RPMI 1640 containing 1 mg of G418 per ml. The mouse fibroblast cell line L929 (clone 430) stably transfected with full-length CD95 (29) was maintained in 10% FCS–RPMI 1640 containing 10 mM HEPES and 500 μg of hygromycin B per ml. The MCF7-Fas cells were maintained in 10% FCS–RPMI 1640 containing 200 μg of G418 per ml and 150 μg of hygromycin B per ml. Unless otherwise stated in the figure legends, adherent cells were detached by trypsination.

Antibodies and reagents. The monoclonal antibody against FADD was purchased from Transduction Laboratories (San Diego, Calif.). The rabbit polyclonal anti-CD95 (C20) and horseradish peroxidase (HRPO)-conjugated goat anti-rabbit immunoglobulin G (IgG) were purchased from Santa Cruz Biotech-

* Corresponding author. Mailing address: The Ben May Institute for Cancer Research, University of Chicago, 924 E. 57th St., Chicago, IL 60637. Phone: (773) 702-4728. Fax: (773) 702-3701. E-mail: MPeter@ben-may.bsd.uchicago.edu.

nologies (Santa Cruz, Calif.). The C15 monoclonal antibody (MAb) recognizes the p18 subunit of caspase 8 (31), and anti-APO-1 (anti-CD95) is an agonistic MAb (IgG3, κ) recognizing an epitope on the extracellular part of CD95 (44). The HRPO-conjugated goat anti-mouse IgG1 and IgG2b were from Southern Biotechnology Associates (Birmingham, Ala.). The transferrin receptor (TfR) antibody (clone B3/25) was obtained from Roche (Indianapolis, Ind.). The fluorescein isothiocyanate (FITC)-conjugated anti-human CD19 MAb (mouse IgG1) was obtained from Ancell Corp. (Bayport, Minn.). All other chemicals used were of analytical grade and were purchased from Sigma (St. Louis, Mo.), Molecular Probes (Eugene, Oreg.), or Calbiochem (San Diego, Calif.).

DISC analysis by Western blotting. A total of 10^7 SKW6.4 or H9 cells were treated with 1 μg of anti-CD95 per ml for 5 min or for the times indicated at 37°C and then lysed in lysis buffer (30 mM Tris-HCl [pH 7.5], 150 mM NaCl, 2 mM EDTA, 1 mM phenylmethylsulfonyl flouride [PMSF], protease inhibitor cocktail [Sigma], 1% Triton X-100, 10% glycerol) (stimulated condition). The CD95 DISC was then immunoprecipitated for 2 h at 4°C with protein A-Sepharose (Sigma). After immunoprecipitation, the beads were washed five times with 1 ml of lysis buffer. For Western blotting, immunoprecipitates were separated by SDS-PAGE (12% polyacrylamide) and transferred to Hybond nitrocellulose membrane (Amersham, Piscataway, N.J.), blocked with 2% bovine serum albumin (BSA) in phosphate-buffered saline (PBS)-Tween (0.05% Tween 20) for 1 h, washed with PBS-Tween, and incubated with the primary antibody in PBS-Tween for 16 h at 4°C. Blots were then incubated with HRPO-conjugated secondary antibody diluted 1/20,000 in PBS-Tween. After being washed with PBS-Tween, the blots were developed by the enhanced chemiluminescence (ECL) method according to the manufacturer's protocol (Amersham).

Induction of apoptosis and cytotoxicity assay. A total of 10^5 cells in 200 μl of medium were incubated in 96-well plates (Corning, Inc., Corning, N.Y.) in the absence or presence of increasing concentrations of lantrunculin A (Ltn A) for 1 h prior to anti-CD95 stimulation. Cells were stimulated with 1 μg of anti-CD95 per ml (unless otherwise stated) or 1 μg of LZ-CD95L per ml at 37°C by incubation for 16 h. Quantification of DNA fragmentation, as a measure of apoptosis, was carried out by nuclear staining with propidium iodide as previously described (32).

Flow cytometric analysis of mitochondrial membrane potential ($\Delta\Psi_m$). To measure $\Delta\Psi_m$, anti-CD95 (2 μg/ml)-treated or untreated SKW6-vec or SKW6-Bcl-2 cells (5×10^5/ml) were incubated with 5 μg of JC-1 (5, 5′, 6, 6′-tetrachloro-1, 1′, 3, 3′-tetraethylbenzimidazolylcarbocyanine iodide) per ml (Molecular Probes). The analysis was performed as previously described (33).

Caspase activity assay. Caspase 8 activity was determined from cell lysates as follows. Cells were stimulated for the indicated times with 1 μg of anti-CD95 per ml. Lysates from 10^6 cells were incubated in cleavage buffer containing 40 μM amino trifluoromethyl coumarin (AFC)-labeled caspase 8-specific peptide IETD for 1 h at 37°C. Caspase activity was determined with a microplate fluorescence reader with a 400-nm excitation filter and 508-nm emission filter. Values of unstimulated cells were taken as background and subtracted from those obtained with stimulated cells. We have recently established that under the conditions used, caspase 8 activity is measured without any appreciable cross-reactivity by effector caspases such as caspase 3 (39).

Detection of CD95 aggregates. To analyze ligand-dependent SDS-stable CD95 microaggregates, 10^6 cells were stimulated with 1 μg of anti-CD95 per ml for 20 min at 37°C. Cells were washed once with PBS and lysed in lysis buffer (50 mM HEPES [pH 7.4], 150 mM NaCl, 10 mM NaF, 10 mM iodoacetamine, 200 μM Na_3VO_4, 1% NP-40). Postnuclear supernatants were analyzed by SDS-PAGE (8% polyacrylamide), and CD95 was detected with the antibody C20.

Internalization assay and immunofluorescence. To monitor the fate of CD95 after stimulation, 10^6 cells/ml were treated with 1 μg of anti-CD95 per ml for 45 min on ice. Unbound antibody was removed by washing with medium at 4°C. Cells were then stained with 1 μg of FITC-conjugated goat anti-mouse IgG per ml for 45 min on ice. Next, cells were washed, warmed, and kept at 37°C for the indicated time points to trigger CD95 stimulation or were kept on ice (time [t] = 0). In some experiments, FITC-conjugated anti-CD95 antibody was used as indicated in the figure legends. After stimulation, cells were adhered to immunofluorescence slides (Polysciences, Warrington, Pa.) precoated with poly-L-lysine (Sigma) and fixed in acetone-methanol (1:1) for 5 min at room temperature. Slides were washed with PBS, rinsed with tap water, mounted with Vectashield (Vector Laboratories, Burlingame, Calif.), and visualized with a Zeiss Axiovert S100 fluorescence microscope equipped with an Axiocam digital camera or with a confocal microscope (Zeiss, LSM 510).

For ligand stimulation, cells were treated with 1 μg of LZ-CD95L per ml for 45 min on ice and stimulated at 37°C as described above. After stimulation, cells were adhered to immunofluorescence slides (Polysciences) precoated with poly-L-lysine (Sigma) and fixed in acetone-methanol (1:1) for 5 min at room temperature. Fixed cells were stained with anti-CD95L antibody (clone G247–4) (Pharmingen, San Diego, Calif.) followed by goat anti-mouse FITC (1:200 dilution in PBS). After staining, slides were washed with PBS and mounted with Vectashield (Vector Laboratories). For costaining with the endocytic marker transferrin receptor (TfR), cells were stained for CD95 as described above, fixed, and then incubated with the anti-TfR antibody (IgG1) (1:200 dilution in PBS) for 45 min. After washing, a Texas red-labeled goat anti-mouse IgG1 antibody (which did not cross-react with the anti-CD95 antibody [IgG3]) was applied and incubated for 45 min.

To distinguish between surface and internalized CD95, 10^6 cells/ml were incubated with 1 μg of FITC-conjugated anti-CD95 antibody per ml for 45 min on ice. After being washed, the cells were resuspended in 37°C medium and incubated at 37°C for the indicated times or kept on ice (time 0). Cells were then resuspended in 300 μl of cold 2% BSA–PBS, stained with Texas red-conjugated goat anti-mouse IgG for 30 min on ice, washed, and resuspended in serum-free medium. The cells were then plated for 5 min at 37°C on poly-L-lysine (Sigma)-coated slides and fixed in methanol-acetone (1:1). Slides were washed and rinsed with water, and coverslips were mounted with Vectashield mounting medium. For quantification of internalization, 100 cells for each condition per cell line were counted by fluorescence microscopy. Cells with 50% or more of CD95 structures stained only green (FITC–anti-CD95) were scored as having internalized the receptor.

Cholesterol depletion studies. SKW6.4 or H9 cells were pretreated with the following cholesterol-depleting agents: 1 μg of filipin per ml, 10 μg of nystatin per ml, or 2 mM methyl-β-cyclodextrin in serum-free medium for 1 h at 37°C. Thereafter, DISC formation and CD95 clustering were analyzed as described above. For induction of apoptosis, cells were pretreated with the cholesterol-depleting agents as described above and incubated with increasing concentrations of anti-CD95 for 9 h (cells in serum-free medium) or for 16 h (cells in serum-containing medium). Apoptosis was quantified by DNA fragmentation by nuclear staining with propidium iodide as previously described (32).

Electron microscopy. For electron microscopy analysis, 3×10^6 cells were resuspended in 300 μl of medium and stained with 6 μg of anti-CD95 antibody for 45 min at 4°C. The cells were then washed and stained with 3 μg of 20-nm-diameter gold particle-conjugated goat anti-mouse IgG (Ted Pella, Inc., Redding, Calif.) for 1 h at 4°C. Cells were washed and kept on ice (t = 0) or resuspended in warm medium and incubated at 37°C for 20 min. After incubation, cells were washed with serum-free medium followed by PBS and fixed with 2% glutaraldehyde buffered with 0.1 M Na cacodylate (pH 7.35) for 10 to 15 min at room temperature. Fixed cells were gently centrifuged, and excess fixative was removed and replaced. Fresh fixative was added to the tube without disturbing the pellet or cell layer, and fixation was continued for 10 min at room temperature. The tube was then transferred to 4°C and centrifuged at 10,000 × g for 10 min to create a tight pellet. This pellet was then stored overnight at 4°C until further processing. Portions of the pellet were washed several times with 0.1 M Na cacodylate (pH 7.35) and postfixed for 1 h on ice in freshly prepared 1% osmium tetroxide–1% potassium ferrocyanide–0.1 M Na cacodylate (pH 7.4). After being washed, cells were stained en bloc in 2% uranyl acetate dehydrated through a graded series of ethanol and embedded in Epon resin. Sixty- to 70-nm-thick sections were cut with a Reichert Ultracut-E microtome and stained for 5 min with 1.5% uranyl acetate, followed by 10 min in Reynolds lead citrate. Samples were visualized with a JEOL Philips CM-120 electron microscope operated at 60 kV.

RESULTS

Formation of the DISC precedes CD95 receptor redistribution. According to the current model of CD95 signaling, binding of either the CD95 ligand (CD95L) or an agonistic antibody induces aggregation of CD95 followed by a conformational change in its cytoplasmic domain that results in formation of the DISC. In this model, receptor clustering would precede formation of the DISC. We have previously shown that recruitment of FADD and caspase 8 in SKW6.4 cells to the DISC can be observed after a few seconds (22, 31). Furthermore it was recently shown that CD95 receptor capping can be observed very early after triggering CD95 (6, 9). To test which of the two events—formation of the DISC or CD95 surface clustering—happens first, we incubated SKW6.4 cells with anti-CD95. We then monitored redistribution of CD95 over a wide range of time from seconds up to 60 min of

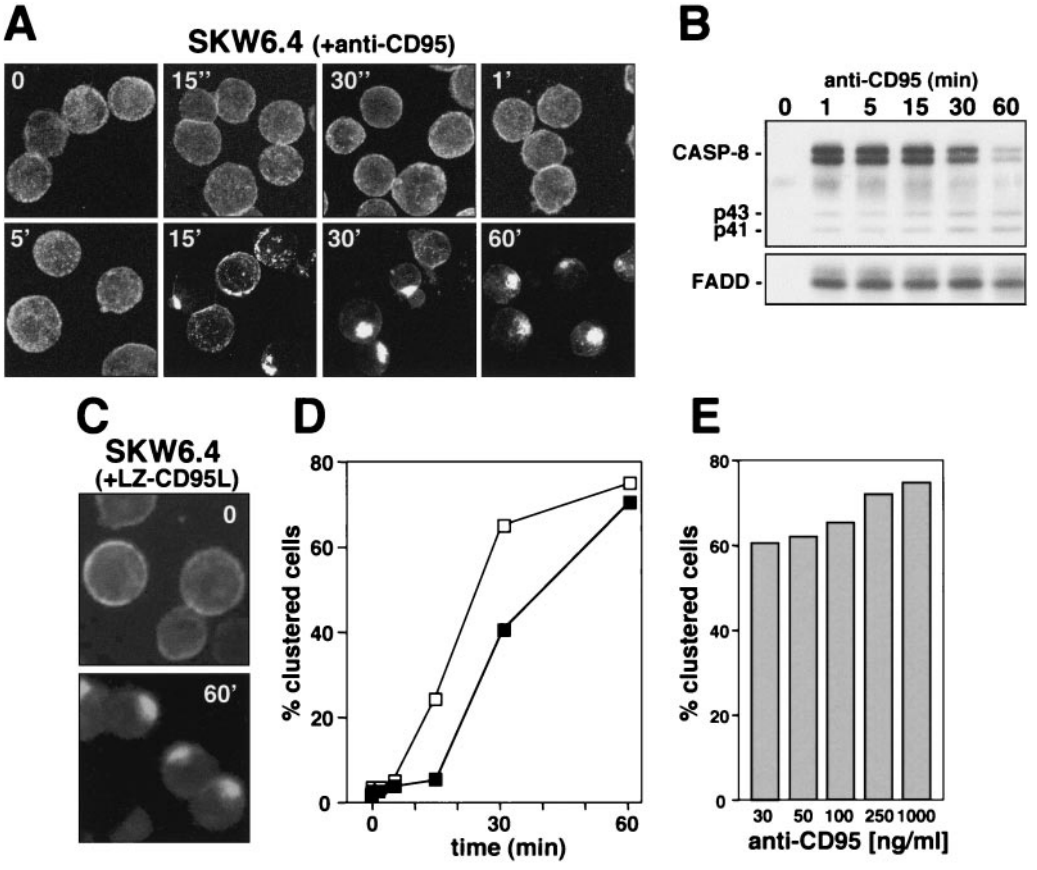

FIG. 1. Ligand-induced DISC formation and clustering of CD95. (A) SKW6.4 cells were incubated with an FITC-conjugated anti-CD95 antibody for 45 min on ice ($t = 0$). Cells were then washed and warmed to 37°C and analyzed after the indicated times. After incubation, cells were attached to poly-L-lysine-coated slides and fixed, and samples were analyzed by confocal laser scanning microscopy in the following way: 20 z-sections of each sample (0.5 μm apart) were taken and used to generate a 3D image with Zeiss LSM software. Projections of these 3D images are shown. All cells are shown at the same magnification. (B) Analysis of the DISC of SKW6.4 cells stimulated with anti-CD95 for the indicated times. Migration positions of procaspase 8 (CASP-8), the caspase 8 cleavage intermediates p43 and p41, and FADD are shown. (C) SKW6.4 cells were treated with 1 μg of LZ-CD95L per ml for 45 min on ice and then stimulated for 60 min at 37°C. Receptor redistribution was determined by staining fixed cells with anti-CD95L antibody followed by FITC-conjugated goat anti-mouse antibody. (D) SKW6.4 cells were treated with 1 μg of either anti-CD95 (□) or LZ-CD95L (■) per ml for different times as described for panel A, and cells were scored for clustering. One hundred cells per condition were counted in duplicate, and the mean is shown. (E) SKW6.4 cells were treated with different amounts of anti-CD95 for 60 min, and clustering of CD95 was quantified as in panel D.

stimulation. Changes in receptor distribution were monitored after stimulating the cells with an FITC-conjugated anti-CD95 antibody (Fig. 1A). Stimulation was stopped by addition of ice-cold PBS and fixation of cells after attaching them to poly-L-lysine-coated slides. To best visualize the formation of small surface patches on whole cells, which may precede formation of receptor caps, we generated two-dimensional projections of three-dimensional images generated by taking 20 z-sections from each slide by using a confocal microscope (Fig. 1A). No significant changes in CD95 distribution were detectable prior to 15 min of stimulation. At 15 min, both receptor patches and receptor clusters were detectable. Almost all cells showed clustering of CD95 after 30 min of stimulation. Following 60 min of incubation with anti-CD95 antibody, the staining on virtually all SKW6.4 cells had changed to a punctate pattern that was so highly clustered, the outline of the cells was difficult to see (Fig. 1A, last panel, bottom row). In a parallel experiment, efficient binding of FADD and caspase 8 to the activated receptor was detected 1 min after receptor triggering (Fig. 1B), which was consistent with our previous reports, in which we showed that formation of the DISC in many cells is detectable seconds after receptor triggering (22, 31).

Clustering of CD95 was also detected when SKW6.4 cells were induced to apoptose by addition of a trimerizing leucine zipper-tagged version of the CD95 ligand (LZ-CD95L) (Fig. 1C), showing that this effect was not limited to the anti-CD95 antibody. A kinetic analysis confirmed that formation of receptor clusters could not be detected prior to 15 min with either the anti-CD95 or the LZ-CD95L (Fig. 1D). Since it was suggested that high antibody concentrations might make CD95 artificially cluster (9), we quantified clustering at different concentrations of anti-CD95. The clustering of CD95 did not depend on the concentration of the stimulating antibody, since clustering could be detected with as little as 30 ng of anti-CD95 per ml (Fig. 1E). The staining of the cells was more intense at higher antibody concentrations, however (data not shown), and we therefore used 1 μg of anti-CD95 per ml for all further experiments.

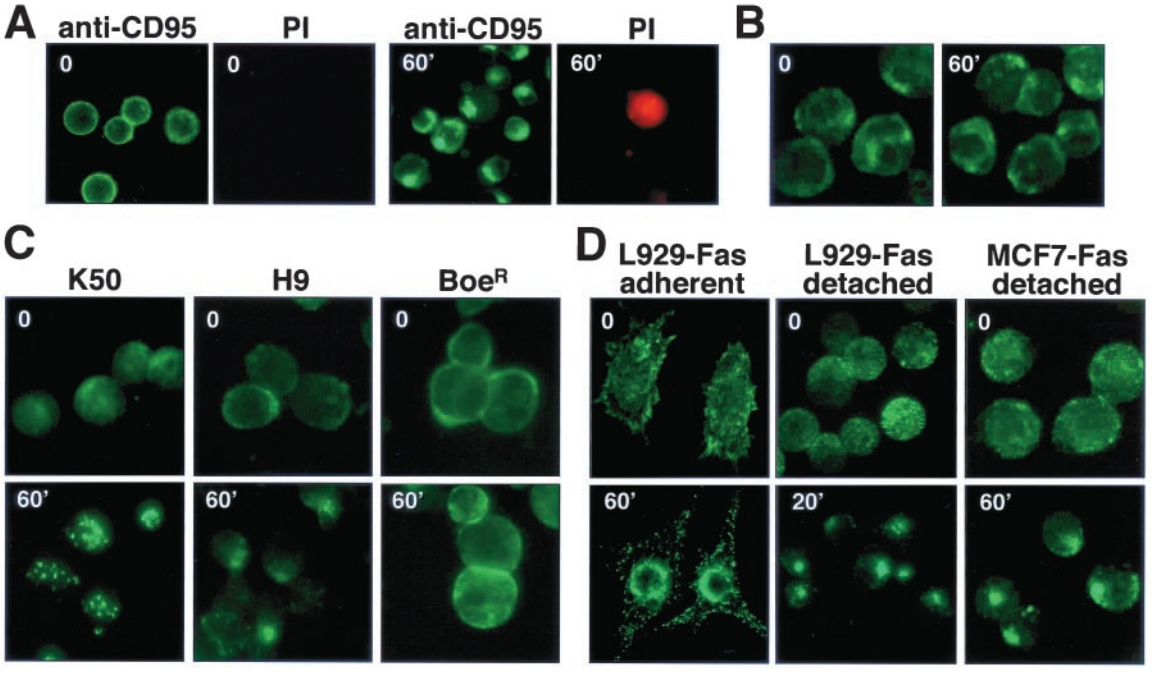

FIG. 2. Clustering of CD95 is a specific and general effect. (A) Living SKW6.4 cells were treated with FITC-conjugated anti-CD95 and incubated for 60 min on ice (time 0) or for 60 min at 37°C (60′). After stimulation, cells were counterstained with propidium iodide (PI) and analyzed by fluorescence microscopy. (B) To establish specificity of the internalization of CD95, K50 cells were incubated with 1 μg of anti-CD95 per ml for 0 or 60 min and after fixation were stained for CD19 with an FITC-conjugated anti-CD19 mouse MAb. (C and D) CD95 clustering on lymphoid (C) and nonlymphoid (D) cells. Receptor clustering of K50, H9, Boe^R, detached L929-Fas, and detached MCF7-Fas cells was performed as follows. Cells were incubated with anti-CD95 followed by FITC-conjugated goat anti-mouse IgG, each for 45 min on ice ($t = 0$). Cells were then warmed to 37°C and analyzed after the indicated times. After incubation, cells were attached to poly-L-lysine-coated slides and fixed, and samples were analyzed by fluorescence microscopy. Stimulated cells are shown at the same magnification as unstimulated cells. Adherent L929-Fas cells were grown on Polyprep poly-L-lysine slides (Sigma) to 70% confluency and transferred to ice-cold medium. Directly, FITC-conjugated anti-CD95 was added, and cells were incubated for 45 min on ice. After being washed in medium, CD95 clustering was induced by transfer of slides to 37°C medium and incubation for 60 min. After fixation, all cells were analyzed by fluorescence microscopy.

Stimulation-induced clustering is specific for CD95 and can be detected in a variety of different cells. Although clustering of CD95 was a late event when compared to formation of the DISC, most cells displaying CD95 clustering were viable, since they excluded the viability dye propidium iodide (Fig. 2A). This experiment also demonstrated that the clustering of CD95 that we detected was not a fixation artifact, since it was observed in living cells after addition of a directly FITC-conjugated anti-CD95 antibody to SKW6.4 cells in culture medium (Fig. 2A).

To confirm that CD95-induced clustering was specific for CD95, we tested whether the surface distribution of CD19, which has previously been shown to cluster in a stimulation-dependent fashion (27), was affected by stimulating CD95 (Fig. 2B). We did not detect a redistribution of CD19 on K50 cells (the Burkitt's lymphoma cell BL-60, stably expressing exogenous human CD95). A control staining of cells for CD95 confirmed that, in this experiment, CD95 did cluster (data not shown).

Since our data are in contradiction to two recent reports that detected clustering of CD95 as early as 30 s after receptor triggering (6, 9), we tested other cell lines to exclude the possibility that the effect was limited to SKW6.4 cells. We found similar kinetics of CD95 clustering in the lymphoid cell lines K50 and H9 (Fig. 2C) and in two cell lines of nonlymphoid origin, L929 and MCF7, both transfected with human CD95 (Fig. 2D). In most cases, maximal CD95 clustering was detected 60 min after triggering. CD95 clustering peaked at 20 min only in detached L929-Fas cells. In none of the cell lines could clustering be observed earlier than 5 min of stimulation with either anti-CD95 or LZ-CD95L (data not shown). CD95 did not cluster at all on one cell line, Boe^R, which expresses large quantities of CD95 on the cell surface and is resistant to CD95-mediated apoptosis (11, 33) (Fig. 2C, last column), again confirming that clustering of CD95 was not artificially induced by adding a cross-linking antibody. This result also suggested that clustering of CD95 was an active process that does not occur in a cell line that is resistant to CD95-mediated apoptosis.

A redistribution of CD95 was also observed in adherent L929-Fas cells (Fig. 2D, first column). However, we found detached L929-Fas cells to be much more sensitive to CD95-mediated apoptosis, and under these conditions, the effect of receptor clustering was more pronounced. The same was true for MCF7 cells stably expressing CD95 (data not shown) (Fig. 2D, right column). Again, the clustering effect of CD95 was not caused by the fixation method, since it was also observed in living L929-Fas cells stimulated with directly FITC-labeled an-

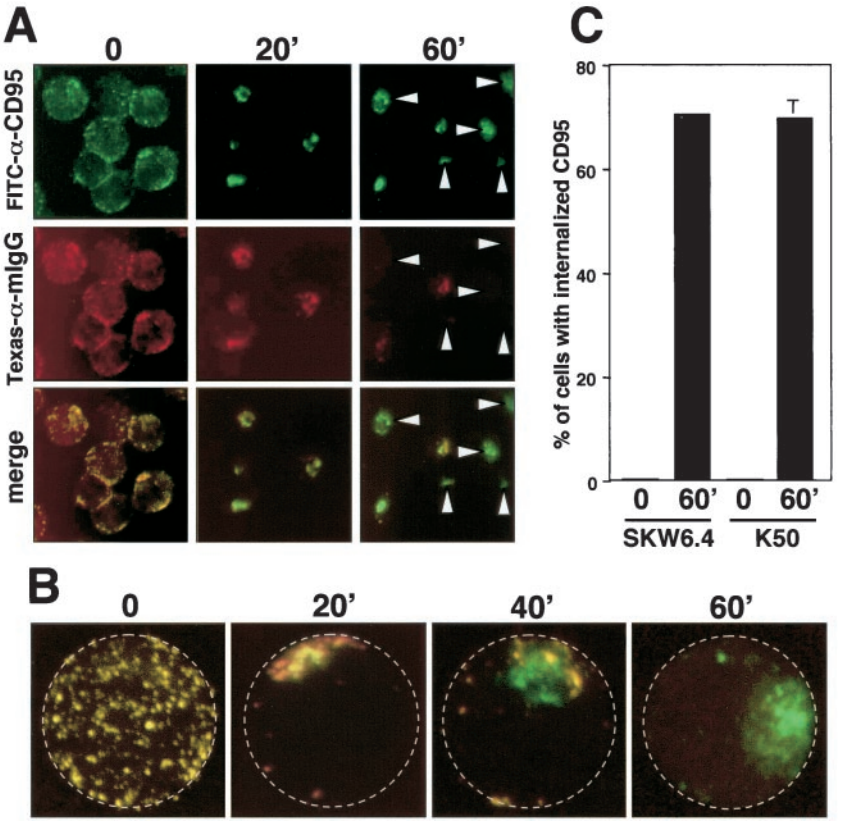

FIG. 3. Stimulation-dependent internalization of CD95. (A) SKW6.4 cells were incubated with FITC-conjugated anti-CD95 for 45 min on ice followed by incubation at 37°C for the indicated time. After washing, cells were stained with Texas red-conjugated goat anti-mouse IgG (αmIgG) and then transferred onto poly-L-lysine-coated slides, fixed, and analyzed by fluorescence microscopy as described in Materials and Methods. Arrowheads point to cells that did not stain with the secondary antibody and therefore have fully internalized CD95. (B) 2D projections of 3D movies of SKW6.4 cells treated as in panel A. For orientation, the plasma membrane is labeled by a stippled circle. (C) Quantification of CD95 internalization at time point 0 and after stimulation of K50 and SKW6.4 cells for 60 min. The number of cells with 50% or more of CD95 internalized was determined as described in Materials and Methods. The experiment was done in triplicate, and the mean values with standard deviations are shown. The numbers of propidium iodide-positive cells following the incubation at 37°C were 8% for SKW6.4 and 6% for K50, respectively.

ti-CD95 (Fig. 2D). In summary, stimulation of all tested cell lines with either anti-CD95 or LZ-CD95L resulted in intense clustering of CD95 that in all cases followed formation of the DISC, revealing an unexplained delay between formation of the DISC and clustering of CD95.

Ligand-induced clustering of CD95 is followed by receptor internalization. In many of the cell lines tested, the punctate pattern of CD95 labeling after ligation appeared to be cytoplasmic rather than clustered on the cell surface. In adherent L929-Fas cells, the observed juxtanuclear staining was particularly indicative of receptor internalization (Fig. 2D). Internalization of CD95 has not yet been reported. A fluorescence-activated cell sorting-based assay as well as many of the typical methods to quantify of receptor internalization (20) proved unreliable in the case of CD95, due to its intense aggregation properties (data not shown). We therefore developed a method to qualitatively determine whether CD95 was on the cell surface or intracellular and to quantify this effect by counting single cells. To this end, living cells were incubated with directly FITC-conjugated anti-CD95 and incubated for different times to induce receptor clustering. After washing, cells were stained with Texas red-conjugated goat anti-mouse IgG. Surface expression was then evaluated by fluorescence microscopy after fixing the cells (Fig. 3A). At the zero time point, CD95 was evenly distributed on the surface of the cells. Both the green (all CD95) and the red (only surface CD95) completely colocalized, indicating that CD95 was at the cell surface. After 20 min, CD95 formed clusters, and at the applied resolution, all clusters were stained in red with the goat anti-mouse antibody, indicating that most CD95 was at the cell surface. At 60 min, however, the majority of the cells showed only a green staining, indicating that CD95 on these cells was inaccessible from the cell surface and suggesting that it had been internalized (arrowheads in Fig. 3A). To further test for the intracellular localization of activated CD95, we used a confocal microscope to generate three-dimensional (3D) images of these cells. In Fig. 3B, 2D projections of such 3D images of representative cells are shown at different stages of CD95 internalization. It is apparent that during the course of the incubation, CD95 moved from the cell surface (red and green = yellow staining) to the interior of the cell (green staining). We then used this assay to quantify the extent of CD95 internalization in different cell lines (Fig. 3C). After 60

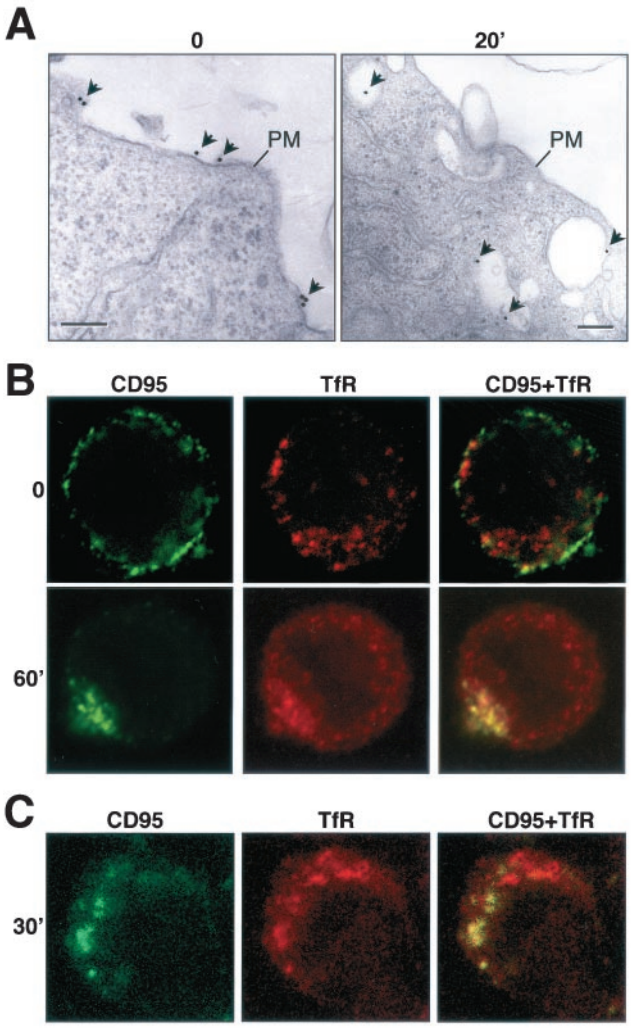

FIG. 4. Colocalization of CD95 with the endosomal marker TfR. (A) Electron microscopic analysis of MCF7-Fas cells stimulated for 0 or 20 min with anti-CD95 and goat anti-mouse IgG covalently labeled with 20-nm-diameter colloidal gold particles. PM, plasma membrane. Gold particles are indicated with arrows. The bar represents 200 nm. (B and C) Detached MCF7-Fas (B) and SKW6.4 (C) cells were treated with anti-CD95 and stimulated for the indicated times at 37°C as described in Fig. 2C. CD95 was detected with an FITC-conjugated goat anti-mouse antibody (green). To detect TfR after CD95 staining and fixation, cells were stained with an anti-TfR antibody followed by Texas red-conjugated goat anti-mouse IgG1 antibody (red). Stainings were analyzed by confocal microscopy. The extent of internalization of MCF7-Fas cells shown in panel B was 80%.

min, approximately 70% of the SKW6.4 and K50 had internalized CD95.

Internalized CD95 is directed to an endosomal pathway. To test whether CD95 is internalized through endocytosing vesicles, we performed an electron microscopic analysis of MCF7-Fas cells (Fig. 4A). After detaching cells, apoptosis and receptor internalization were induced by addition of anti-CD95, directly followed by addition of goat anti-mouse IgG conjugated to 20-nm-diameter gold particles and incubation for 20 min at 37°C. The electron micrographs confirmed that in these cells, CD95 can be found in intracellular vesicles early after receptor triggering (Fig. 4A). To test whether CD95 was internalized through an endosomal pathway, a costaining for CD95 and TfR, as a marker for early endosomes, was performed and evaluated by confocal microscopy. In unstimulated MCF7-Fas cells, CD95 was on the cell surface and did not colocalize with TfR (Fig. 4B, upper row). After 60 min of stimulation, however, most of the CD95 was found in TfR-positive endosomal vesicles (Fig. 4B, lower row). Similar analysis showed that 30 min after addition of anti-CD95 to SKW6.4 cells, intracellular vesicles stained positive for both CD95 and TfR, again indicating that CD95 was internalized and transported to endosomes (Fig. 4C). These data suggest that stimulation of CD95 results in internalization of the receptor-ligand complex, which is then directed towards an endosomal pathway.

Efficient formation of the DISC and internalization of CD95 both require actin filaments. The actin inhibitor Ltn A has been demonstrated to effectively inhibit ligand-dependent internalization of a number of surface receptors (15, 18). Treatment of SKW6.4 cells with Ltn A prior to CD95-induced activation resulted in dramatic changes in the CD95 staining pattern from small, dispersed puncta to a single large spot on each cell (Fig. 5A). Ltn A treatment also somewhat increased the evenness of surface staining of the CD95, which remained distributed around the cell surface (Fig. 5A), suggesting that Ltn A also partially inhibited CD95 clustering at the cell surface. To determine whether internalization of CD95 was affected by Ltn A, cell surface localization of CD95 was tested by the same method used in Fig. 3B (Fig. 5B). A quantification of the internalization of CD95 in Ltn A-treated SKW6.4 and K50 cells confirmed that, in the majority of the cells, CD95 was still at the cell surface (Fig. 5C). These data indicate that Ltn A inhibited the internalization of activated CD95. To test whether the actin dependence of clustering of CD95 involved myosins, we pretreated cells with the myosin inhibitor 2-3-butanedione monoxime (BDM). BDM did not affect CD95 clustering, suggesting that only actin filaments, and not the actin-myosin motor function, are required for this process (data not shown).

Monodansylcadaverine (MDC) has recently been shown to inhibit internalization of the related receptor tumor necrosis factor receptor I (TNF-RI) (36). We therefore tested whether MDC had any effect on the clustering and internalization of CD95. MDC did not prevent clustering of CD95 (Fig. 5A) or its internalization (data not shown). Consistent with the recent report, it also did not inhibit CD95 signaling (data not shown), suggesting that CD95 and TNF-RI internalize through a different mechanism.

The finding that the internalization of CD95 could be prevented by inhibiting actin filaments prompted us to test whether Ltn A would also have an effect on the formation of the DISC and subsequent generation of active caspase 8. Ltn A inhibited recruitment of FADD (Fig. 5D) and caspase 8 (data not shown) to the DISC of SKW6.4 and H9 cells, resulting in severely reduced activation of caspase 8 at the two concentrations of Ltn A used in the experiments (Fig. 5E). To test whether inhibition of receptor clustering or internalization would affect signaling through CD95, we induced apoptosis in SKW6.4 and H9 cells by stimulation with either anti-CD95 or CD95L in the presence of increasing concentrations of Ltn A

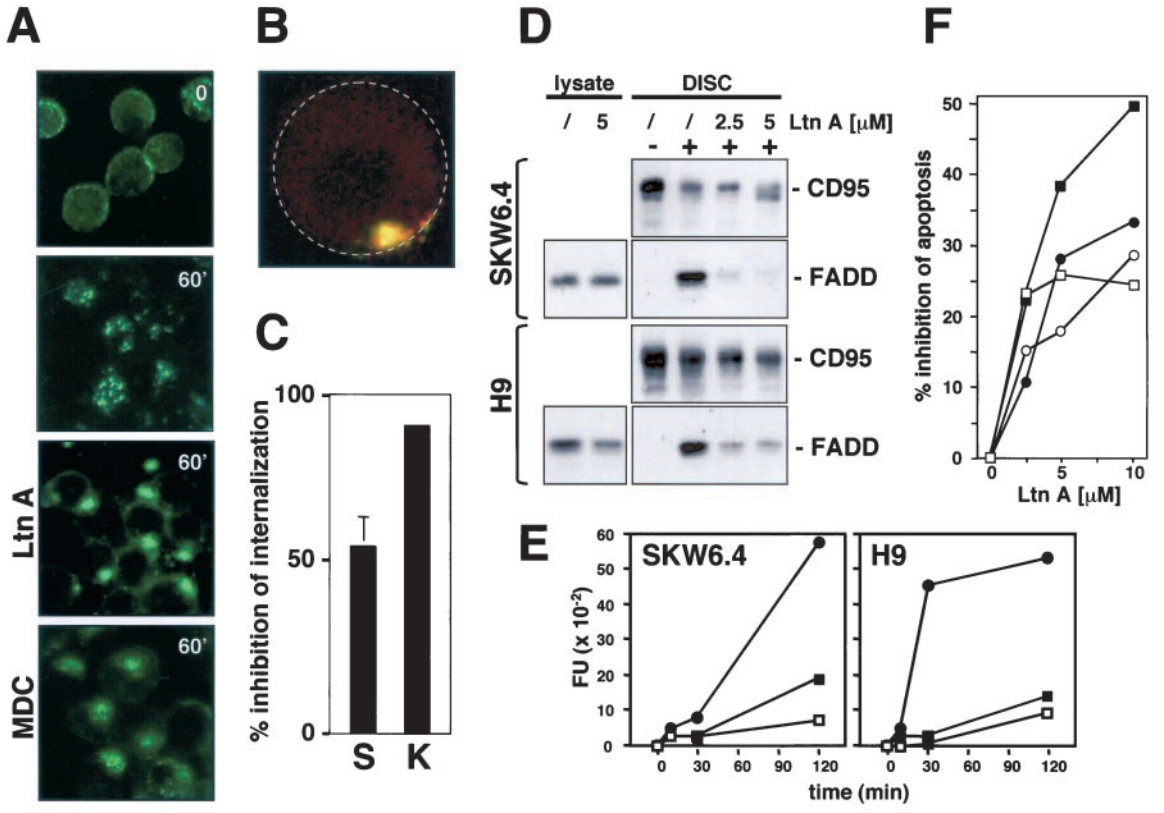

FIG. 5. Actin filaments are required for CD95 DISC formation and receptor internalization. (A) SKW6.4 cells were left untreated or pretreated with 2.5 μM Ltn A or 100 μM MDC for 1 h at 37°C. Cells were then treated with anti-CD95 and left unstimulated (time 0) or stimulated for 60 min (60′) at 37°C as described in Fig. 2C. Samples were analyzed by fluorescence microscopy. (B) 2D projection of a 3D analysis of an Ltn A-treated SKW6.4 cell stimulated for 1 h at 37°C as described for panel A. Cells were analyzed as described in Fig. 3B. The yellow color indicates that CD95 is at the cell surface. For orientation, the outline of the cell is indicated by a stippled circle. (C) Quantification of inhibition of CD95 internalization on SKW6.4 (S) and K50 (K) cells by 5 μM Ltn A. The number of cells with 50% or more of CD95 internalized was determined as described in Materials and Methods. The experiment was done in triplicate, and the mean values with standard deviations are shown. (D) SKW6.4 or H9 cells were pretreated with Ltn A (2.5 or 5.0 μM) for 1 h at 37°C. CD95 was immunoprecipitated from either 10^7 untreated or anti-CD95-treated (5 min) SKW6.4 or H9 cells. Immunoprecipitates were subjected to SDS-PAGE (12% polyacrylamide) and immunoblotted with anti-FADD MAb and anti-CD95 C20. Migration positions for each protein are indicated. Cell lysates equivalent to 40 μg of protein were subjected to SDS-PAGE (12% polyacrylamide) and immunoblotted with anti-FADD antibody. (E) SKW6.4 and H9 cells were treated with 1 μg of anti-CD95 per ml for different periods of time in the absence (●) or presence of LtnA (2.5 μM [■] or 5.0 μM [□]). Caspase 8 activity was analyzed by cleavage of the fluorogenic substrate IETD-AFC. This result was confirmed by a Western blot analysis that demonstrated reduced activation of caspase 8 in Ltn A-treated cells (data not shown). FU, fluorescence units. (F) SKW6.4 (circles) and H9 (squares) cells were preincubated with the indicated concentrations of Ltn A for 1 h and then incubated for 16 h with 1 μg of anti-CD95 (open symbols) or LZ-CD95L (solid symbols) per ml. After incubation, cells were harvested and analyzed by flow cytometry for DNA fragmentation with nuclear staining with propidium iodide. Nontoxic concentrations of Ltn A were chosen after titration of Ltn A to toxic levels. The data represent the percentage of decrease of apoptosis in the presence of Ltn A. The percentages of specific apoptosis in the absence of Ltn A were 58% (56%) and 70% (80%) for SKW6.4 and H9 cells treated with anti-CD95 (LZ-CD95L), respectively. The experiment is representative of three independent experiments.

and quantified DNA fragmentation (Fig. 5F). Ltn A inhibited CD95-mediated apoptosis, resulting in up to 50% inhibition of DNA fragmentation (Fig. 5F). These data suggest that an intact actin cytoskeleton is required for formation of the DISC as well as for internalization of CD95 in these cells, but do not exclude the possibility that actin is also involved in processes further downstream in the pathway.

Clustering of CD95 is an active process that depends on activation of caspase 8 at the DISC. The results observed with the apoptosis-resistant Boe^R cells and the kinetics of CD95 clustering in many cells suggested that binding of anti-CD95 antibodies or CD95L to CD95 alone is not sufficient to induce receptor clustering. To test whether the initiation of the caspase cascade at the DISC was required to induce clustering of CD95, we tested BJAB cells stably expressing a dominant-negative version of FADD (FADD-DN) that is recruited to the CD95 DISC, but is unable to bind to procaspase 8 (5). Triggering CD95 in the BJAB-vec cells resulted in clustering of CD95 (Fig. 6A). In contrast, FADD-DN-transfected BJAB cells did not show any signs of CD95 clustering. These data suggest that caspase activation is required to induce receptor clustering. In the CD95 pathway, caspases are activated at two steps, upstream or downstream of mitochondria. We have previously shown that the type I SKW6 cells expressing Bcl-2 activate caspases in a way that is absolutely independent of mitochondrial functions (32). Like SKW6.4 cells, these transfectants responded to triggering through CD95 with receptor clustering (Fig. 6B) and internalization (data not shown). The

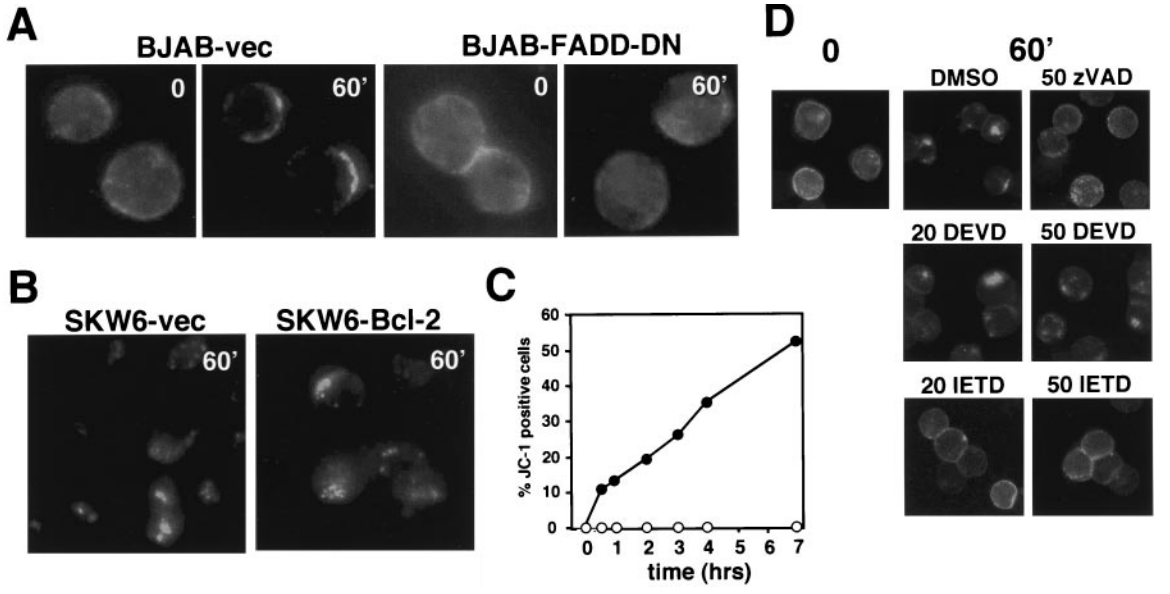

FIG. 6. CD95 receptor clustering and internalization require caspase 8 activation. (A) Induction of CD95 clustering on BJAB vector transfectants or BJAB cells expressing FADD-DN as described in Fig. 2C. (B) Induction of CD95 clustering of SKW6 vector-transfected cells or SKW6 cells stably expressing Bcl-2 as described in Fig. 2C. (C) SKW6-vec (●) or SKW6-Bcl-2 (○) transfectants were treated with 1 μg of anti-CD95 per ml for different periods of time. $\Delta\Psi_m$ was determined as described in Materials and Methods. (D) MCF7-Fas cells were treated with either 20 or 50 μM caspase inhibitor zVAD-fmk (polycaspase inhibitor), zDEVD-fmk (caspase 3 or 7), or zIETD-fmk (caspase 8). After treatment, cells were incubated with anti-CD95 and kept on ice (time 0) or stimulated for 60 min (60′) at 37°C. Receptor localization was determined as described in Fig. 2C.

intensity and kinetics of this process were identical to those of the vector-transfected control (SKW6-vec). In contrast to the vector control, we could not detect a drop in the mitochondrial transmembrane potential ($\Delta\Psi_m$) in the SKW6-Bcl-2 cells (Fig. 6C), demonstrating that Bcl-2 fully prevented mitochondrial dysfunction in these cells. We can therefore exclude a mitochondrial contribution to the clustering and internalization of CD95 in these cells, suggesting that a DISC-generated caspase was regulating receptor clustering. To test whether caspase 8 regulates CD95 clustering, we used MCF7-Fas cells, which do not express caspase 3 and activate only caspase 8 within the first 4 h of receptor stimulation (39). In MCF7-Fas cells, CD95 efficiently clustered following stimulation (and was internalized [Fig. 4A and B]) (32). We again chose to analyze detached MCF7 cells, since we found that they activate caspase 8 much more efficiently than adherent cells (data not shown). Addition of the poly-caspase inhibitor zVAD-fmk prevented receptor internalization in these cells. To test whether an IETD (caspase 8)- and not a DEVD (caspase 3)-cleaving activity was involved in receptor internalization, we compared the effects of zIETD-fmk with those of zDEVD-fmk (Fig. 6D). The caspase 8-selective inhibitor blocked receptor internalization at 20 μM, whereas the caspase 3-selective inhibitor did not inhibit this process at concentrations as high as 50 μM. Inhibition of caspase 8 also efficiently inhibited receptor clustering in other cells, such as SKW6.4, K50, and H9 (data not shown). Taken together, all data suggest that early activation of caspase 8 at the DISC regulates clustering of CD95, which is a prerequisite for receptor internalization in these cells.

CD95 signaling in type I cells is independent of lipid rafts. It has recently been shown that CD95 signals via ceramide-rich lipid rafts in the type II cells, Jurkat cells and hepatocytes (6, 9). Pretreatment of these cells with the cholesterol-depleting reagents nystatin, filipin, and methyl-β-cyclodextrin disrupted membrane microdomains, resulting in blockage of CD95 signaling. To determine the effects of these reagents on the caspase 8-dependent clustering defined in our study, we treated SKW6.4 cells with these three reagents and tested receptor clustering (Fig. 7A). Cholesterol depletion had no effect on the caspase 8-dependent formation of CD95 clusters. In addition we tested the effects of these reagents on the activation of caspase 8 in the DISC (Fig. 7B). Again we found no effect of cholesterol depletion on CD95 signaling. Since it was suggested that clustering of CD95 was dependent on the concentration of stimulus (9), we determined the titer of the anti-CD95 antibody from 0 to 1 μg/ml and quantified DNA fragmentation in the presence of these three cholesterol-depleting reagents (Fig. 7C). We observed no effect of these treatments on CD95 sensitivity, suggesting that lipid rafts do not play a major role in CD95 signaling in the cells used in our study.

The earliest event during CD95 signaling is actin- and caspase 8-independent formation of SDS-stable CD95 microaggregates, which precedes DISC formation. Recruitment of both FADD and caspase 8 to the DISC is independent of caspase activity, since zVAD-fmk did not inhibit this step (Fig. 8A). However, preincubation of SKW6.4 cells with zVAD-fmk prevented activation of caspase 8 within the DISC, because the formation of the caspase 8 cleavage intermediates p43 and p41 was almost completely inhibited. At the same time, inhibition of caspases almost completely blocked the ligand-induced clustering of CD95 in SKW6.4 cells (Fig. 8B). The data suggest

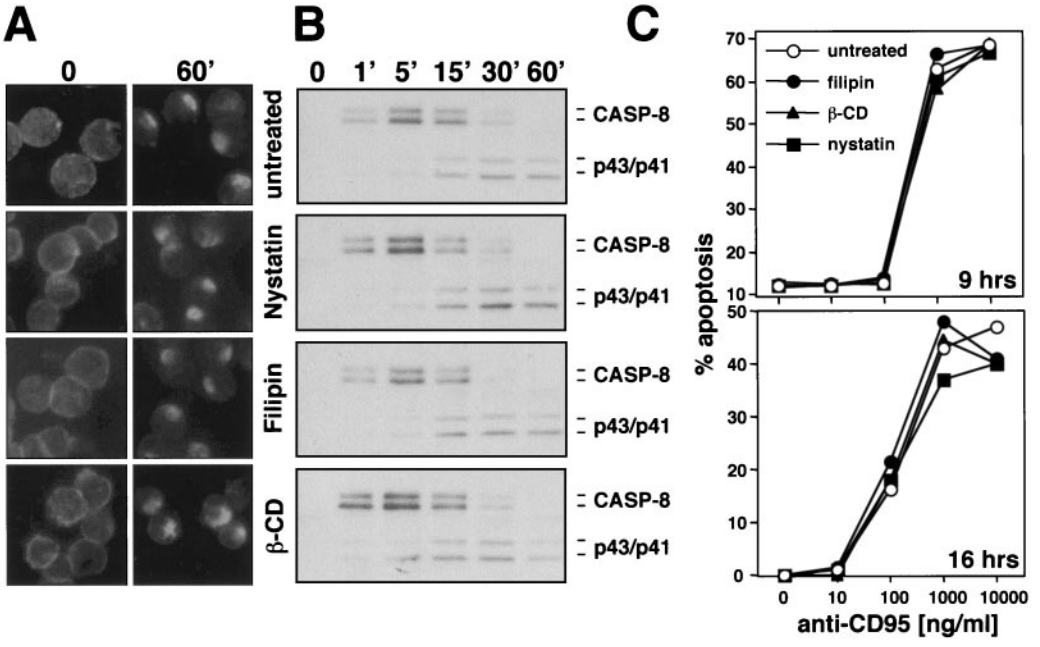

FIG. 7. CD95 signaling on SKW6.4 cells cannot be inhibited by destruction of lipid rafts (A) SKW6.4 cells were left untreated or were pretreated with 10 μg of nystatin per ml, 1 μg of filipin per ml, or 2 mM methyl-β-cyclodextrin (β-CD) for 1 h at 37°C. Cells were then treated with anti-CD95 and left unstimulated (time 0) or were stimulated for 60 min (60′) at 37°C as described in Fig. 1A. Samples were analyzed by fluorescence microscopy. (B) Analysis of the DISC of 10^7 SKW6.4 cells treated for different times with the same reagents as in panel A was performed as described in Fig. 1B. (C) Titration of anti-CD95 onto SKW6.4 cells in the presence of the indicated reagents used at the same concentrations as in panel A. Cells were treated in either serum-free medium for 9 h or serum-containing medium for 16 h, and DNA fragmentation was quantified as described in Materials and Methods. Similar data were obtained when H9 cells were tested in the same way (data not shown).

that caspase 8 activation is required for the receptor clustering. To determine whether inhibition of caspase 8 also inhibits receptor internalization, we pretreated SKW6.4 and H9 cells with zIETD-fmk and quantified internalization of CD95 60 min after addition of anti-CD95 (Fig. 8C). This treatment resulted in a very efficient inhibition of CD95 internalization, suggesting that caspase 8 regulates both CD95 clustering and its internalization.

One of the earliest events after triggering of CD95 is the formation of high-molecular-weight SDS-stable aggregates, which can be found seconds after receptor engagement (11). In contrast to the receptor clusters detectable by immunofluorescence microscopy, the early formation of these aggregates does not require actin filaments or activity of caspases, since neither Ltn A nor zVAD-fmk inhibited this step (Fig. 8D). Formation of SDS-stable microaggregates was also unaffected by pretreating cells with any of the three cholesterol-depleting agents used in Fig. 7 (data not shown). Formation of these aggregates is therefore directly caused by the binding of the anti-CD95 antibody or CD95L and does not depend on a signal emanating from CD95. Our data allow us to distinguish and molecularly order at least four different membrane-proximal CD95 signaling events: formation of SDS-stable aggregates, formation of the DISC, and clustering and internalization of CD95.

DISCUSSION

In this study, we have ordered the earliest events of CD95-mediated signaling. We demonstrate that upon binding of an agonistic anti-CD95 antibody or CD95L, CD95 forms clusters and internalizes in all tested type I cells. Stimulation of CD95 is sufficient to induce microaggregation of the receptor; however, when actin filaments are disrupted, such stimulation is insufficient to induce formation of a DISC that produces large quantities of active caspase 8. We have therefore discovered that both actin and active caspase 8 act in a positive feedback loop that contributes to the signal initiation phase of CD95, resulting in efficient generation of active caspase 8 at the DISC typical for type I cells. Formation of the DISC is therefore an active process, and some DISC component must link CD95 to the actin cytoskeleton. Cortical actin filaments can be linked to surface receptors via linker proteins of the ERM (ezrin-radixin-moesin) family (3, 45). It has recently been demonstrated that CD95 directly associates and colocalizes with ezrin in certain cells (25), providing a direct link between CD95 and actin. However, how triggering of CD95 affected ezrin association or at what step in the CD95 pathway actin was important was not tested.

Involvement of the actin filament system in the ligand-induced internalization of many receptors is well documented (28). Ltn A, a toxin isolated from a Red Sea sponge, disrupts microfilament organization in cultured cells by binding to monomeric G-actin in a 1:1 complex at submicromolar concentrations (38) and is a widely used inhibitor of receptor-mediated endocytosis (15, 18). Ltn A has been shown to inhibit CD95-mediated apoptosis in certain cells (42), suggesting that actin is involved in signaling through CD95. Recently, we reported a role for actin in regulating apoptosis sensitivity of

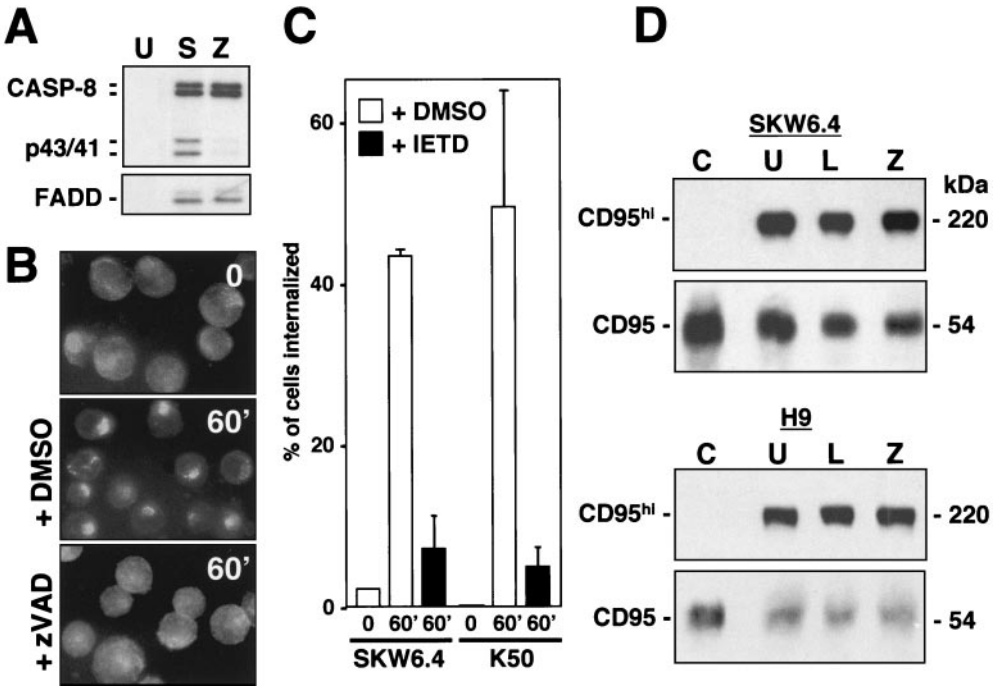

FIG. 8. Formation of SDS-stable CD95 microaggregates is independent of actin and caspase activity. (A) CD95 was immunoprecipitated from either 10^7 unstimulated (U) or anti-CD95 stimulated (5 min) SKW6.4 cells that were left untreated (S) or that had been pretreated with 50 μM zVAD-fmk (Z). Immunoprecipitates were subjected to SDS-PAGE (12% polyacrylamide) and immunoblotted with anti-caspase 8 and anti-FADD antibodies. p43 and p41 are cleavage intermediates of activated caspase 8. DISC formation was also unaffected by zVAD-fmk when cells were stimulated with anti-CD95 for 60 min (data not shown). (B) SKW6.4 cells were incubated with anti-CD95 and left unstimulated (time 0) or stimulated for 60 min (60′) at 37°C as described in Fig. 2C after pretreatment with 50 μM zVAD-fmk. 0, mock treatment with 0.5% dimethyl sulfoxide (DMSO) alone. Samples were analyzed by fluorescence microscopy. (C) Ligand-induced internalization of SKW6.4 cells or K50 cells untreated or pretreated with zIETD-fmk for 60 min was quantified as described in Fig. 3C. (D) A total of 10^6 SKW6.4 and H9 cells stimulated with anti-CD95 (20 min) were left untreated (U) or had been pretreated with 5 μM Ltn A (L) or 50 μM zVAD-fmk (Z). Unstimulated cells were analyzed as a control (C). Cell lysates were subjected to SDS-PAGE (10% polyacrylamide) and immunoblotted with anti-CD95 (C20) antibody. $CD95^{hi}$ corresponds to SDS-stable CD95 microaggregates migrating at around 220 kDa during SDS-PAGE.

restimulated Th2 cells (46). However, under these conditions, polymerized actin impaired CD95-mediated apoptosis by inhibiting lateral diffusion of the receptor and consequently cytochalasin D-sensitized apoptosis-resistant Th2 cells. In contrast to this role of the actin cytoskeleton in maintaining the CD95 apoptosis resistance of restimulated Th2 cells, we now report a general role for actin in regulating formation of the DISC and internalization of CD95 in all tested apoptosis-sensitive type I cells.

Formation of the DISC in type I cells is detectable seconds after receptor triggering (22, 31). Since type II cells form almost no DISC, inhibition of actin polymerization does not affect generation of caspase 8 in these cells (data not shown). Consistent with this finding, Ltn A could not completely block generation of active caspase 8 or apoptosis in type I cells. The cells still died with mitochondrial signal amplification, reminiscent of the situation found in type II cells (32).

CD95 has previously been shown to form caps as a result of receptor triggering. In one report, capping of the receptor was shown to occur between 40 and 60 min after triggering, consistent with our data (47). However, two recent reports showed that CD95 caps in a ceramide-dependent fashion as early as 30 s after receptor triggering (6, 9). These two studies were mainly done with type II cells—Jurkat cells and hepatocytes. We did not see a significant difference in the kinetics of CD95 clustering between the type I cells used in our study and the type II Jurkat and CEM cells. However, the CD95 clusters in type II cells were smaller, and clustering could not be inhibited by caspase inhibitors (unpublished results). Localization of CD95 to lipid rafts was required in these studies for efficient signaling. Most of the CD95 receptor clusters detected in our study represent internalized receptor. Only when internalization of CD95 was blocked by treating cells with Ltn A did we detect intense clusters of CD95 on the cell surface (Fig. 5A and B). However, under these conditions recruitment of FADD to the DISC, activation of caspase 8, and the efficiency of apoptosis signaling were all severely impaired (Fig. 5D to F). This is not consistent with the recent reports describing the necessity of recruitment of CD95 and its signaling molecules to clusters in lipid rafts (6, 9). Consequently, pretreatment of cells with the same cholesterol-depleting reagents used in these studies did not affect signaling in the tested cells (Fig. 7).

These discrepancies suggest a different mechanism of signal initiation between type I and type II cells. Our original finding is consistent with this assumption—only type II Jurkat and CEM cells are sensitive to C_2-ceramide-induced apoptosis, whereas the type I SKW6.4 and H9 cells are completely resistant (33)—as well as with our recent finding that type II Jurkat and CEM cells do not internalize CD95 upon stimulation (data not shown). These findings could provide an explanation for

the contradiction with the two recently published reports on CD95 capping. We are currently investigating the differences in receptor clustering and internalization between type I and type II cells. Alternatively, the differences between our study and two recently published reports (6, 9) could be due to differences in the methods and reagents used to trigger CD95 and/or to detect the capped receptor. In these two reports, cells were stimulated with CH11 (IgM) or sCD95L, and capped CD95 on fixed cells was visualized by labeled secondary antibodies. In contrast, we stimulated cells with anti-CD95 (IgG3) or LZ-CD95L. This stimulation also resulted in CD95 receptor clustering in living cells when a primary labeled anti-CD95 antibody was used.

It has been suggested that the use of higher concentrations of CD95-stimulating agents would artificially cluster CD95 on cells (9), producing an unphysiological triggering of CD95. We have set the titer of our anti-CD95 antibody down to 30 ng/ml with no loss in the ability to induce clustering of the receptor after stimulation. Moreover, the fact that clustering of CD95 could completely be prevented by pretreating cells with caspase inhibitors confirms that CD95 clustering in our experiments is an active process that follows the triggering of the receptor and activation of caspase 8. This is also supported by the fact that the CD95 on the $CD95^{high}$-expressing Boe^{R} cells does not form clusters or a DISC (33) and does not internalize (data not shown) regardless of how much antibody is added. We can, however, detect SDS-stable microaggregates in these cells (data not shown) after addition of anti-CD95, confirming that the anti-CD95 binds and triggers aggregation of CD95.

No previously published report has tested whether activated CD95 internalizes after clustering. We now demonstrate that triggering CD95 results in receptor internalization shortly after engagement of the receptor by either anti-CD95 MAb or CD95L. Internalization of CD95 was found in lymphoid and nonlymphoid cells, in suspension as well as in adherent cells. Although stimulation-induced receptor internalization of CD95 has not been previously reported, CD95 can be forced to internalize. It has been shown that the adenoviral proteins E3/10.4K to -14.5K induce internalization of CD95 followed by its lysosomal degradation (7, 43). This mechanism was interpreted as a viral strategy to protect its infected host cell through down-modulation of CD95.

The endocytosis machinery is a complex network of different pathways. Cargo can be endocytosed via clathrin-coated pits, by the clathrin-independent pathway, or through caveolae (21). All of these pathways lead to the appearance of cargo in the peripheral early endosomes. We have not yet observed CD95 in coated vesicles in our transmission electron microscopy analysis. However, internalization of CD95 could be prevented by depleting K^{+}, suggesting a mechanism of internalization that depends on coated pits (data not shown). We detected colocalization of internalized CD95 with the lysosomal marker Lamp-1 in some but not all cells (data not shown). Future experiments will determine which pathway of endocytosis is used by the internalized CD95 receptor.

Receptor internalization plays an important role in desensitizing cells to specific extracellular signals and in recycling receptor and/or ligand molecules. Down-modulation of receptors on cells that have received a death stimulus, although seemingly counterproductive, may actually be important physiologically. CD95L bound to surface CD95 may be harmful to neighboring nonapoptosing cells or to macrophages that attempt to engulf apoptotic cells. It may therefore be advantageous and protective for the organism for an apoptosing cell to internalize the death receptor-ligand complex. Growing evidence suggests that the process of receptor internalization is also required to colocalize activated receptors with downstream signaling molecules (reviewed in reference 4). Internalization of a DISC actively producing caspase 8 may therefore be important for targeting the caspase to its intracellular substrates. Future experiments aim to further dissect the initial CD95 signaling events by separating the DISC formation phase from the internalization phase.

Alternatively, activation of caspase 8 does not invariably lead to apoptosis (23). Therefore cells could receive a rescue signal after triggering of CD95 and the surviving cells could potentially recycle internalized CD95 to the surface. We recently showed that MCF7-Fas cells are protected from apoptosis by stable expression of Bcl-x_L and that none of the cytosolic caspase substrates is cleaved. However, clustering of CD95 and its internalization occurs and can be prevented by pretreating cells with zIETD-fmk (A. Stegh, B. C. Barnhart, A. Algeciras-Schimnich, and M. E. Peter, submitted for publication), suggesting that very small quantities of active caspase 8 are sufficient to initiate this process. The finding that nonapoptosing cells also internalize CD95 after CD95 stimulation also demonstrates that internalization of CD95 is not just an unspecific event due to changes in the membrane of apoptosing cells. The data rather support our model of both clustering and internalization as active processes that are regulated by activation of caspase 8.

It has recently been demonstrated that another member of the death receptor family, TNF-RI, internalizes upon binding to its ligand TNF-α (36). In this report, the authors demonstrated differences between TNF-RI and CD95. Internalization of TNF-RI was inhibited by the transglutaminase inhibitor MDC. Similar to our study, inhibition of internalization of TNF-RI also inhibited apoptosis induction by the receptor. This inhibition was selective for TNF-RI, since, consistent with our data, MDC did not affect CD95 signaling (36; data not shown).

Interestingly, internalization of TNF-RI cannot be prevented by inhibiting caspases (M. Kroenke, personal communication), confirming that the receptors use different mechanisms for internalization. To our knowledge, CD95 is the first receptor the internalization of which requires activation of caspases. The fact that CD19 was not internalized upon triggering of CD95 suggests that CD95 is internalized in a ligand- and caspase-dependent fashion. However, this does not exclude the possibility that surface molecules in general specifically internalize in a caspase-dependent fashion without being directly stimulated. Activation of caspases could trigger clustering and internalization of receptors, including CD95. Such a mechanism could explain how agents that induce apoptosis by activating caspases could cause clustering of CD95 in a ligand-independent fashion, as has been shown for antitumor ether lipids, UV radiation, and the herpes simplex thymidine kinase-ganciclovir suicide gene therapy system (1, 2, 8).

Caspases may not directly regulate the internalization step of CD95 signaling, since caspase activity is already required for

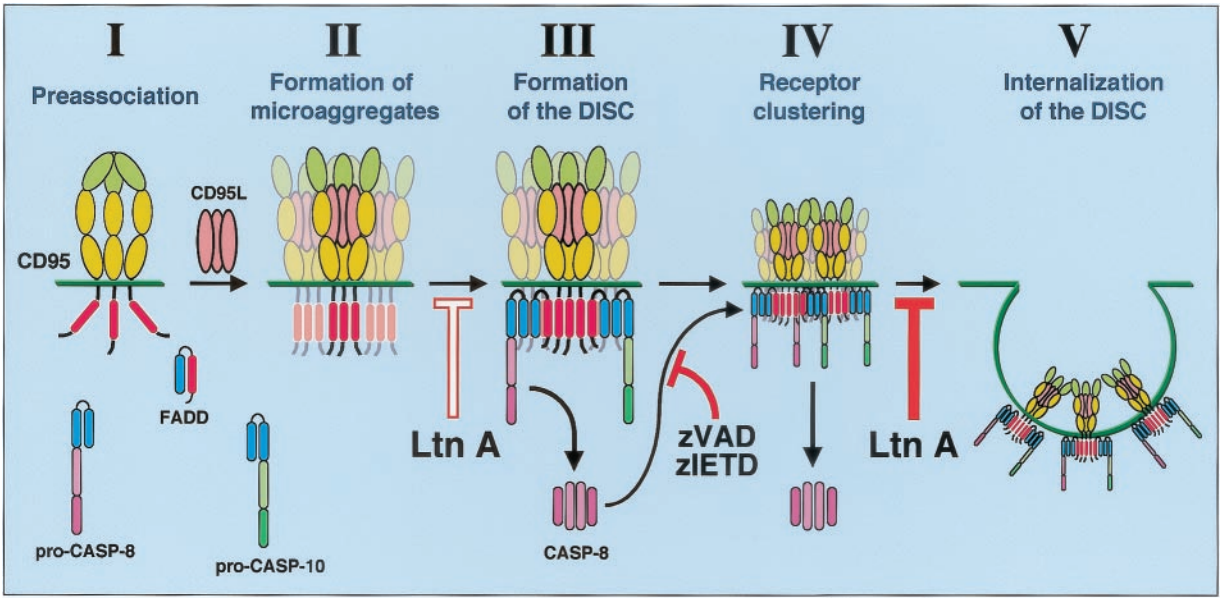

FIG. 9. The membrane-proximal events of CD95 signaling. The signal initiation phase of CD95 can be subdivided into five distinct steps. (I) Ligand-independent receptor preassociation (37). (II) Formation of microaggregates. These submicroscopic microaggregates can be detected as SDS-stable high-molecular-weight CD95 bands in SDS-PAGE (Fig. 8C). (III) Formation of the DISC. This step is dependent on actin filaments, since it can be inhibited by Ltn A (Fig. 5D). DISC components are FADD/Mort1, caspase 8, caspase 10 (unpublished data), and c-FLIP (not shown) (34). (IV) Receptor clustering. CD95 clusters can be seen by fluorescence microscopy. This step depends on generation of active caspase 8 by the DISC and can be efficiently prevented by preincubating cells with either zVAD-fmk or zIETD-fmk (Fig. 6D). Caspase 8 activation is therefore part of a positive feedback loop. (V) Internalization of the DISC. This step again is dependent on actin, since treatment of cells with Ltn A prevents internalization of the clustered receptor (Fig. 5C). Ltn A does not affect type II cells (data not shown), indicating that the actin-dependent steps are reduced or absent and explaining why type II cells form very little DISC. Blue domains, DED; red domain, DD. The N-terminal PLAD in CD95 is shown in a different green tone.

formation of CD95 surface clusters. Caspase-induced surface clustering could, however, be a prerequisite for internalization of CD95. Our data favor caspase 8 as the caspase regulating this process, because MCF7-Fas cells, which do not express caspase 3 and mainly activate caspase 8 during the first 4 h after CD95 triggering (39), very efficiently internalize CD95. Furthermore, the caspase 8-selective inhibitor zIETD-fmk inhibited receptor internalization much more efficiently than the caspase 3- or 7-selective inhibitor zDEVD-fmk. Ligand-induced surface clustering of CD95 followed by internalization of the CD95 DISC may therefore depend on proteolytic degradation of a death substrate by DISC-generated caspase 8, resulting in remodeling of cortical actin. It is unlikely that gelsolin, a regulator of actin dynamics that has been shown to be a caspase substrate (12), triggers the events described in this report, because gelsolin was shown to be cleaved by caspase 3, which is not expressed in MCF7 cells.

Our study has revealed that the signal initiation by CD95 is much more complex than originally expected. The process can now be described as five distinct steps (Fig. 9). First, CD95 resides on the plasma membrane in a preassociated form through its PLAD domain (Fig. 9, step I). Homophilic association through this domain was shown to be a requisite step in recruiting signaling proteins to the DD (37). The next step in CD95 signaling is formation of SDS-stable CD95 microaggregates, as detected by SDS-PAGE (Fig. 9, step II). This step is not yet dependent on activation of caspases or actin filaments, since it is not inhibited by zIETD-fmk or Ltn A. At this stage, the aggregates cannot be seen as receptor clusters by immunofluorescence microscopy and must therefore occur locally as microaggregates. Both kinetics and inhibitor studies suggest that the next step in CD95 signaling is formation of the DISC (Fig. 9, step III). In type I cells, the first recruitment of FADD can be detected seconds after receptor engagement (8). This step requires actin filaments, since it can substantially be inhibited by Ltn A. DISC formation precedes formation of receptor clusters that can be detected by immunofluorescence analysis (Fig. 9, step IV). Surface clusters of CD95 can be observed beginning at 15 min, followed by internalization, which in most cells is complete at around 30 to 60 min after binding of anti-CD95 antibody or CD95L. After pretreatment with Ltn A, surface clustering seems to be intensified, likely due to the absence of actin filaments and the inhibition of receptor internalization. Inhibition of caspase 8 completely blocks CD95 surface clustering, demonstrating that it is an active process and providing an explanation for the delay between formation of the DISC and CD95 surface clustering. The final step of the events at the plasma membrane involves internalization of the activated DISC (Fig. 9, step V). This step, as with many other cases of receptor internalization, can be blocked by inhibiting actin with Ltn A. Future work will be directed at elucidating the mechanism by which actin facilitates formation of the DISC, the identification of the caspase 8 substrate that regulates clustering of CD95, the physiological role of the internalization of activated CD95, and the contribution of the internalized DISC to the execution of apoptosis once inside the cell.

ACKNOWLEDGMENTS

We thank P. Krammer for providing us with anti-APO-1, H. Walczak for his generous gift of LZ-CD95L, and M. Jäättelä and A. Strasser for providing us with the MCF7-Fas and SKW6-Bcl-2 cells, respectively. We also thank E. Williamson of the University of Chicago Cancer Research Center Electron Microscopy Core.

This work was funded by NIH grant GM61712. A. A.-S. is supported by Cancer Biology Training Program 5T32CA09594. B.C.B. is supported by Molecular and Cell Biology Training grant 5T32GM07183.

REFERENCES

1. **Aragane, Y., D. Kulms, D. Metze, G. Wilkes, B. Poppelmann, T. A. Luger, and T. Schwarz.** 1998. Ultraviolet light induces apoptosis via direct activation of CD95 (Fas/APO-1) independently of its ligand CD95L. J. Cell Biol. **140:**171–182.
2. **Beltinger, C., S. Fulda, T. Kammertoens, E. Meyer, W. Uckert, and K. M. Debatin.** 1999. Herpes simplex virus thymidine kinase/ganciclovir-induced apoptosis involves ligand-independent death receptor aggregation and activation of caspases. Proc. Natl. Acad. Sci. USA **96:**8699–8704.
3. **Bretscher, A.** 1999. Regulation of cortical structure by the ezrin-radixin-moesin protein family. Curr. Opin. Cell Biol. **11:**109–116.
4. **Ceresa, B. P., and S. L. Schmid.** 2000. Regulation of signal transduction by endocytosis. Curr. Opin. Cell Biol. **12:**204–210.
5. **Chinnaiyan, A. M., C. Tepper, L. Lou, K. O'Rourke, M. A. Seldin, F. Kischkel, S. Hellbardt, P. H. Krammer, M. E. Peter, and V. M. Dixit.** 1996. FADD/MORT1 is a common mediator of Fas/APO-1- and tumor necrosis factor-induced apoptosis. J. Biol. Chem. **271:**4961–4965.
6. **Cremesti, A., F. Paris, H. Grassme, N. Holler, J. Tschopp, Z. Fuks, E. Gulbins, and R. Kolesnick.** 2001. Ceramide enables Fas to cap and kill. J. Biol. Chem. **276:**23954–23961.
7. **Elsing, A., and H. G. Burgert.** 1998. The adenovirus E3/10.4K-14.5K proteins down-modulate the apoptosis receptor Fas/Apo-1 by inducing its internalization. Proc. Natl. Acad. Sci. USA **95:**10072–10077.
8. **Gajate, C., R. I. Fonteriz, C. Cabaner, G. Alvarez-Noves, Y. Alvarez-Rodriguez, M. Modolell, and F. Mollinedo.** 2000. Intracellular triggering of Fas, independently of FasL, as a new mechanism of antitumor ether lipid-induced apoptosis. Int. J. Cancer **85:**674–682.
9. **Grassme, H., A. Jekle, A. Riehle, H. Schwarz, J. Berger, K. Sandhoff, R. Kolesnick, and E. Gulbins.** 2001. CD95 signaling via ceramide-rich membrane rafts. J. Biol. Chem. **276:**20589–20596.
10. **Kamitani, T., H. P. Nguyen, and E. T. Yeh.** 1997. Activation-induced aggregation and processing of the human Fas antigen. Detection with cytoplasmic domain-specific antibodies. J. Biol. Chem. **272:**22307–22314.
11. **Kischkel, F. C., S. Hellbardt, I. Behrmann, M. Germer, M. Pawlita, P. H. Krammer, and M. E. Peter.** 1995. Cytotoxicity-dependent APO-1 (Fas/CD95)-associated proteins form a death-inducing signaling complex (DISC) with the receptor. EMBO J. **14:**5579–5588.
12. **Kothakota, S., T. Azuma, C. Reinhard, A. Klippel, J. Tang, K. Chu, T. J. McGarry, M. W. Kirschner, K. Koths, D. J. Kwiatkowski, and L. T. Williams.** 1997. Caspase-3-generated fragment of gelsolin: effector of morphological change in apoptosis. Science **278:**294–298.
13. **Kuwana, T., J. J. Smith, M. Muzio, V. Dixit, D. D. Newmeyer, and S. Kornbluth.** 1998. Apoptosis induction by caspase-8 is amplified through the mitochondrial release of cytochrome c. J. Biol. Chem. **273:**16589–16594.
14. **Lacronique, V., A. Mignon, M. Fabre, B. Viollet, N. Rouquet, T. Molina, A. Porteu, A. Henrion, D. Bouscary, P. Varlet, V. Joulin, and A. Kahn.** 1996. Bcl-2 protects from lethal hepatic apoptosis induced by an anti-Fas antibody in mice. Nat. Med. **2:**80–86.
15. **Lamaze, C., L. M. Fujimoto, H. L. Yin, and S. L. Schmid.** 1997. The actin cytoskeleton is required for receptor-mediated endocytosis in mammalian cells. J. Biol. Chem. **272:**20332–20335.
16. **Li, H., H. Zhu, C. J. Xu, and J. Yuan.** 1998. Cleavage of BID by caspase 8 mediates the mitochondrial damage in the Fas pathway of apoptosis. Cell **94:**491–501.
17. **Lindsten, T., A. J. Ross, A. King, W. X. Zong, J. C. Rathmell, H. A. Shiels, E. Ulrich, K. G. Waymire, P. Mahar, K. Frauwirth, Y. Chen, M. Wei, V. M. Eng, D. M. Adelman, M. C. Simon, A. Ma, J. A. Golden, G. Evan, S. J. Korsmeyer, G. R. MacGregor, and C. Thompson.** 2000. The combined functions of proapoptotic Bcl-2 family members bak and bax are essential for normal development of multiple tissues. Mol. Cell **6:**1389–1399.
18. **Lunn, J. A., H. Wong, E. Rozengurt, and J. H. Walsh.** 2000. Requirement of cortical actin organization for bombesin, endothelin, and EGF receptor internalization. Am. J. Physiol. Cell. Physiol. **279:**C2019–C2027.
19. **Luo, X., I. Budihardjo, H. Zou, C. Slaughter, and X. Wang.** 1998. Bid, a Bcl2 interacting protein, mediates cytochrome c release from mitochondria in response to activation of cell surface death receptors. Cell **94:**481–490.
20. **Marks, M. S., L. Woodruff, H. Ohno, and J. S. Bonifacino.** 1996. Protein targeting by tyrosine- and di-leucine-based signals: evidence for distinct saturable components. J. Cell Biol. **135:**341–354.
21. **Marsh, M., and H. T. McMahon.** 1999. The structural era of endocytosis. Science **285:**215–220.
22. **Medema, J. P., C. Scaffidi, F. C. Kischkel, A. Shevchenko, M. Mann, P. H. Krammer, and M. E. Peter.** 1997. FLICE is activated by association with the CD95 death-inducing signaling complex DISC. EMBO J. **16:**2794–2804.
23. **Medema, J. P., C. Scaffidi, P. H. Krammer, and M. E. Peter.** 1998. Bcl-x_L acts downstream of caspase-8 activation by the death-inducing signaling complex. J. Biol. Chem. **273:**3388–3393.
24. **Papoff, G., P. Hausler, A. Eramo, M. G. Pagano, G. Di Leve, A. Signore, and G. Ruberti.** 1999. Identification and characterization of a ligand-independent oligomerization domain in the extracellular region of the CD95 death receptor. J. Biol. Chem. **274:**38241–38250.
25. **Parlato, S., A. M. Giammarioli, M. Logozzi, F. Lozupone, P. Matarrese, F. Luciani, M. Falchi, W. Malorni, and S. Fais.** 2000. CD95 APO-1/Fas. linkage to the actin cytoskeleton through ezrin in human T lymphocytes: a novel regulatory mechanism of the CD95 apoptotic pathway. EMBO J. **19:**5123–5134.
26. **Peter, M. E., C. Scaffidi, J. P. Medema, F. Kischkel, and P. H. Krammer.** 1999. The death receptors. Results Probl. Cell Differ. **23:**25–63.
27. **Pulczynski, S., A. M. Boesen, and O. M. Jensen.** 1993. Antibody-induced modulation and intracellular transport of CD10 and CD19 antigens in human B-cell lines: an immunofluorescence and immunoelectron microscopy study. Blood. **81:**1549–1557.
28. **Qualmann, B., M. M. Kessels, and R. B. Kelly.** 2000. Molecular links between endocytosis and the actin cytoskeleton. J. Cell Biol. **150:**F111–F116.
29. **Ratter, F., M. Germer, T. Fischbach, K. Schulze-Osthoff, M. E. Peter, W. Dröge, P. H. Krammer, and V. Lehmann.** 1996. S-adenosylhomocysteine as a physiological modulator of Apo-1-mediated apoptosis. Int. Immunol. **8:**1139–1147.
30. **Rodriguez, I., K. Matsuura, K. Khatib, J. C. Reed, S. Nagata, and P. Vassalli.** 1996. A bcl-2 transgene expressed in hepatocytes protects mice from fulminant liver destruction but not from rapid death induced by anti-Fas antibody injection. J. Exp. Med. **183:**1031–1036.
31. **Scaffidi, C., J. P. Medema, P. H. Krammer, and M. E. Peter.** 1997. FLICE is predominantly expressed as two functionally active isoforms, caspase-8/a and caspase-8/b. J. Biol. Chem. **272:**26953–26958.
32. **Scaffidi, C., S. Fulda, A. Srinivasan, C. Friesen, F. Li, K. J. Tomaselli, K. M. Debatin, P. H. Krammer, and M. E. Peter.** 1998. Two CD95 APO-1/Fas signaling pathways. EMBO J. **17:**1675–1687.
33. **Scaffidi, C., I. Schmitz, J. Zha, S. J. Korsmeyer, P. H. Krammer, and M. E. Peter.** 1999. Differential modulation of apoptosis sensitivity in CD95 type I and type II cells. J. Biol. Chem. **274:**22532–22538.
34. **Scaffidi, C., I. Schmitz, P. H. Krammer, and M. E. Peter.** 1999. The role of c-FLIP in modulation of CD95-induced apoptosis. J. Biol. Chem. **274:**1541–1548.
35. **Scaffidi, C., J. Volkland, I. Blomberg, I. Hoffmann, P. H. Krammer, and M. E. Peter.** 2000. Phosphorylation of FADD/Mort1 at serine 194 and association with a 70 kDa cell cycle regulated kinase. J. Immunol. **164:**1236–1242.
36. **Schütze, S., T. Machleidt, D. Adam, R. Schwandner, K. Wiegmann, M. L. Kruse, M. Heinrich, M. Wickel, and M. Krönke.** 1999. Inhibition of receptor internalization by monodansylcadaverine selectively blocks p55 tumor necrosis factor receptor death domain signaling. J. Biol. Chem. **274:**10203–10212.
37. **Siegel, R. M., J. K. Frederiksen, D. A. Zacharias, F. K. Chan, M. Johnson, D. Lynch, R. Y. Tsien, and M. J. Lenardo.** 2000. Fas preassociation required for apoptosis signaling and dominant inhibition by pathogenic mutations. Science **288:**2354–2357.
38. **Spector, I., N. R. Shochet, Y. Kashman, and A. Groweiss.** 1983. Latrunculins: novel marine toxins that disrupt microfilament organization in cultured cells. Science **219:**493–495.
39. **Stegh, A. H., H. Herrmann, S. Lampel, D. Weisenberger, K. Andrä, M. Seper, G. Wiche, P. H. Krammer, and M. E. Peter.** 2000. Identification of the cytolinker plectin as a major early in vivo substrate for caspase 8 during CD95 and tumor necrosis factor receptor-mediated apoptosis. Mol. Cell. Biol. **20:**5665–5679.
40. **Stennicke, H. R., J. M. Jürgensmeier, H. Shin, Q. Deveraux, B. B. Wolf, X. Yang, Q. Zhou, H. M. Ellerby, L. M. Ellerby, D. Bredesen, D. R. Green, J. C. Reed, C. J. Froelich, and G. S. Salvesen.** 1998. Pro-caspase-3 is a major physiologic target of caspase-8. J. Biol. Chem. **273:**27084–27090.
41. **Strasser, A., A. W. Harris, D. C. Huang, P. H. Krammer, and S. Cory.** 1995. Bcl-2 and Fas/APO-1 regulate distinct pathways to lymphocyte apoptosis. EMBO J. **14:**6136–6147.
42. **Subauste, M. C., M. Von Herrath, V. Benard, C. E. Chamberlain, T. H. Chuang, K. Chu, G. M. Bokoch, and K. M. Hahn.** 2000. Rho family proteins modulate rapid apoptosis induced by cytotoxic T lymphocytes and Fas. J. Biol. Chem. **275:**9725–9733.
43. **Tollefson, A. E., T. W. Hermiston, D. L. Lichtenstein, C. F. Colle, R. A. Tripp, T. Dimitrov, K. Toth, C. E. Wells, P. C. Doherty, and W. S. Wold.** 1998. Forced degradation of Fas inhibits apoptosis in adenovirus-infected cells. Nature **392:**726–730.
44. **Trauth, B. C., C. Klas, A. M. Peters, S. Matzku, P. Möller, W. Falk, K. M.**

Debatin, and P. H. Krammer. 1989. Monoclonal antibody-mediated tumor regression by induction of apoptosis. Science **245:**301–305.
45. **Tsukita, S., and S. Yonemura.** 1999. Cortical actin organization: lessons from ERM ezrin/radixin/moesin. proteins. J. Biol. Chem. **274:**34507–34510.
46. **Varadhachary, A. S., M. Edidin, A. M. Hanlon, M. E. Peter, P. H. Krammer, and P. Salgame.** 2001. Phosphatidylinositol 3′-kinase blocks CD95 aggregation and caspase-8 cleavage at the death-inducing signaling complex by modulating lateral diffusion of CD95. J. Immunol. **166:**6564–6569.
47. **von Reyher, U., J. Strater, W. Kittstein, M. Gschwendt, P. H. Krammer, and P. Möller.** 1998. Colon carcinoma cells use different mechanisms to escape CD95-mediated apoptosis. Cancer Res. **58:**526–534.
48. **Wei, M. C., W.-X. Zong, E. H.-Y. Cheng, T. Lindsten, K. V. Panoutsakopoulou, A. J. Ross, K. A. Roth, G. R. MacGregor, C. B. Thompson, and S. J. Korsmeyer.** 2001. Proapoptotic BAX and BAK: a requisite gateway to mitochondrial dysfunction and death. Science **292:**727–730.
49. **Yin, X. M., K. Wang, A. Gross, Y. Zhao, S. Zinkel, B. Klocke, K. A. Roth, and S. J. Korsmeyer.** 1999. Bid-deficient mice are resistant to Fas-induced hepatocellular apoptosis. Nature **400:**886–891.